한국동력기계공학회지 제9권 제4호 pp.31~38 2005년 11월

# Characteristics on the Thermal and Fluid Flow in the Rectangular Aquarium Basin by Using PIV

# PIV를 이용한 사각수조 내의 온도와 유체 유동 특성

B. H. Kim, Dibyendu Konar, H. M. Jeong and H. S. Chung
김보한 · 디벤듀 코나르 · 정효민 · 정한식

**Key Words** : PIV(Particle Image Velocimetry), Standard k ε turbulence model, FVM(Finite Volume Method)

**Abstract** : 육상 수조식 양식장은 해수를 끌어들여 어류를 기르는 데 사용된다. 본 연구는 사각 수조 내의 다양한 기하학적 관계와 유동에 대한 유동 특성을 도출하였다. 수치해석은 유한 체적법과 SIMPLE 기수법은 수치해석법을 활용하였으며, 비압축성 유체와 3차원 표준 k-ε난류 모델을 적용하였다. 속도 분포, 온도 분포에 대한 정보를 확보하였다. 실험과 수치해석의 결과가 정성적으로 잘 일치함을 보였다. 양식장의 깊이가 증가함에 따라 바닥 쪽의 유동이 더욱 안정됨을 확인하였다. 이는 각종 배설물 등의 정체 현상으로 연결될 수 있음을 확인하였다. 수조내의 온도는 유입구의 초기 온도가 중요하며, Re 수가 증가할수록 온도는 상승하고 유입구의 반대 벽면 근처의 온도가 유입구 보다 증가함을 알 수 있었다.

## 기호 설명

$d$ : 직경
X,Y,Z : 각방향의 길이
x,y,z : 무차원 각 방향 길이 L/X, H/Y, W/Z
H : Y-방향 길이(mm)
L : X-방향 길이(mm)
W : Z-방향 길이(mm)
Re : 레이놀즈 수
$t$ : 두께(mm)
$\rho$ : 밀도 [kg/m$^3$]
$\sigma$ : Prandtl 계수
$\varepsilon$ : 난류 에너지 소산율
$\sigma_k$, $\sigma_\varepsilon$, $C_{\varepsilon 1}$, $C_{\varepsilon 2}$, $C_{\varepsilon 3}$, $C_{\varepsilon 4}$ : 모델 상수

## 첨 자

$i$ , $j$ : 직계 좌표계의 방향

접수일 : 2005년 7월 13일
정한식(책임저자) : 경상대학교 기계항공공학부
E-mail : hschung@gsnu.ac.kr Tel. 055-640-3185
김보한 : 경상대학교 대학원
Dibyendu konar : Indian Institute of Technology, India
정효민 : 경상대학교 기계항공공학부

## 1. INTRODUCTION

These days our coasts have been damaged by the polluted water resulting from the construction of industry on the sea shore, increasing population, and urbanization. As compared with the open sea, an inland sea has a higher pollution level because of entropy ,red tide and the later being surrounded by habitats or industries from all sides. The destruction of ecosystem has lent many problems to aquaculture that raises aquatic products for eating.

The major environmental factors include water temperature, the amount of dissolved oxygen which is a function of the water temperature, salt, CO2, ammonia, PH and amount of nourished salt that are associated with the breeding of the aquaculture because imbalance in these may have effects on the growth of the creatures and lead to their serious diseases.

In the korean aquaculture industry, lefteye flounder (Paralichthys olivaceus) and rock fish (Sebastes schlegeli) are preferred by fishermen on the grounds that the value and better returns, and the latter has advantage of raising the creatures. Nowadays, inland aquafarm uses recirculated sea

water. This implies that to help quickly grow and to be strong enough to get over diseases, the fishes need to have much of melted oxygen and hence better control and maintenance of optimum water temperature is necessary. Recirculated sea water cause many problems. The major problem with this process is increased cost of production associated with cooling down the hot water before recirculating it .Also improper cooling and imbalance in the water contents leads to various diseases to fish.

Several investigations of aquaculture in sea water have been reported. Kim(1997) examined the marine pollutions in view of biology. This biological treatment has no problems in aquaculture industry because the aquarium tank is separated from the water pollution. Partridge (1989) and Sannomiya(1987) examined the swimming structure and behavior of fish in aquarium tank. Takaki et al.(1993) considered the effect of the aquarium tankssize and shape. Generally, the aquaculture equipment has two types of closed and open flow systems. Jeong et al.(1998) reported the flow characteristic by comparing numerical analysis and flow visualization images. Mirashi et al. (1995) examined the effect of water current in the aquaculture environment of the seas. The closed type is the system which the sea water is recirculated again in the aquarium tank. The water in the case of the open flow system is discharged to the sea. Thus, the first system needs more expensive equipment, but this system can save the energy for heating needed by the aquarium tank water in winter season unlike in open systems where the incoming water has to be heated each time and the useful hot water discarded instead of recirculating it. Lee(1994) carried out the experiment of a flow characteristics in the closed aquarium tank. In the design of an aquarium tank, what needs to be emphasized is the aquaculture environments, This means that the wrong design can cause the mass mortality of the breeding fish.

In this paper, we performed a numerical analysis for fluid flow characteristics in an inland aquafarm, and the numerical results are compared with the experimental results by visualization technique with PIV. This paper is intended as an investigation of the flow characteristics in an inland aquafarm, and we will concentrate on the temperature and velocity distributions.

## 2 STUDY METHODS

### 2.1 Experimental Study

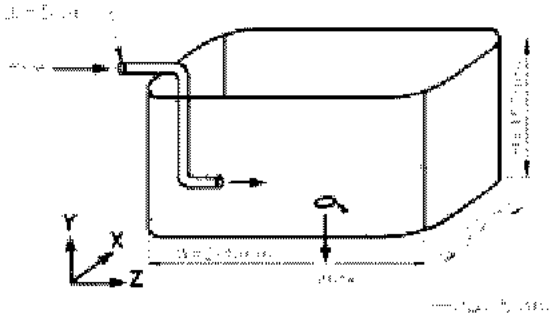


**Fig. 1 Schematic diagram for numerical model**

Fig. 1 shows the schematic diagram of the numerical analysis model. The geometry of an inland aquafarm model is W×H×L=200mm×200m ×40mm. where L is the height of the water level in the model .The height of the model is 150mm. This model consisted of one inlet and one outlet pipe with diameter d=5mm. The height of the inlet pipe to the model aquafarm is 35mm. The dimensions of an actual aquafarm is 5m×5m×1.1-1.3 m where 1,1-1.3m is the height of water level in the actual aquafarm. The height of the actual aquafarm tank is 3.75-4m. It can be seen that our model has been scaled down from the original model by 25 times.

Fig. 2(a) and (b) shows the schematic diagram and photograph of the experimental apparatus. The experimental test model has a rectangular type top opening which has rounded four corner. The top surface is opened with an outside temperature of 10℃. The working fluid used by water at 20℃ and the incoming flow rate was set to Re=2.12×103. The bottom and side walls were

covered with black paint to achieve good particle image by CCD camera. The laser source was an Argon-Ion laser with 490mW.

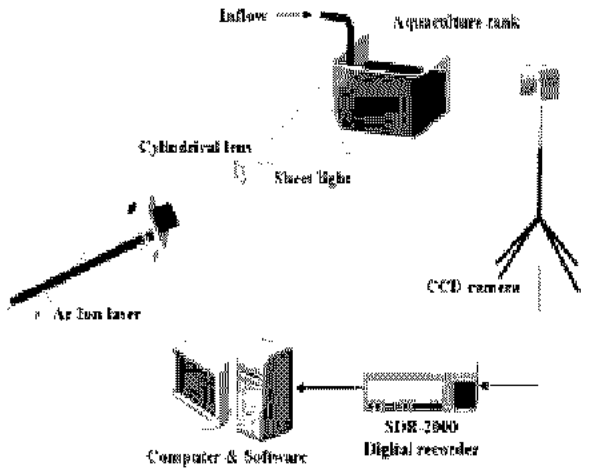


(a) Schematic diagram of experimental apparatus

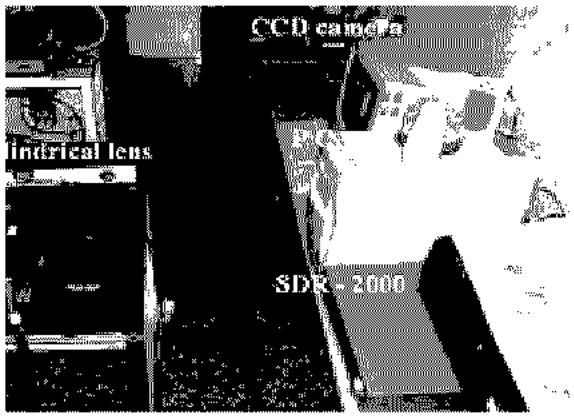


(b) Photograph of experimental apparatus

**Fig. 2 Schematic diagram and Photograph**

**Table 1 Experimental conditions for PIV measurement**

| Item | Specification |
|---|---|
| Image grabber | DT3155(640×480 pixel, B & W) |
| Light source | 750mW, Ar Ion Laser |
| Particle seed | PVC(Poly Vinyl Chloride : 200㎛) |
| Working fluid | Water(20℃) |
| Sheet light | Cylinderical Lens |
| Image recorder | SDR 2000 |
| Computer | Intel Pentium Ⅲ PC(800MHz) |
| Frame number for time averaged | 200 Frames |
| Identification | Two Frame Gray Level Cross Correlation Algorithm |

Table 1 shows the apparatus used in the present experimental study. The particle tracers are PVC(Poly Vinyl Chloride) whose average diameter is 200㎛. The CCD camera, model CV-M50, was used for image capturing. The number of images is 200 frames to get an average image. The cross-correlation algorithm was adopted to calculate the coefficients from two consecutive images. 200 consecutive image frames were captured successively and digitized with a frame grabber into arrays of 640×480 pixels.

### 2.2 Numerical analysis

Three-dimensional incompressible steady-state (water pumped in = water taken out through the withdrawal pipe) Navier-Stokes equations were used to predict the internal flow and heat transfer characteristics. The standard k-ε turbulence model is generally used in the analysis of a turbulent flow field. The SIMPLE(Semi-Implicit Method for Pressure-Linked Equations) solution algorithm for correcting the pressure field was used, as explained in Parankar(1980).

**Table 2 Flow chart of PIV processing**

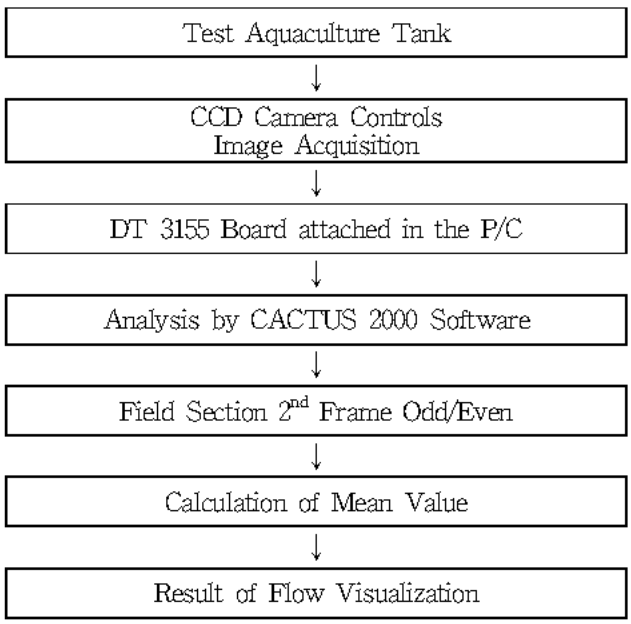


This is mainly suitable for steady state flows and is stable for undistorted grid systems. Its virtue is that it is computationally efficient,

generally requiring less CPU effort per iteration than other more hybrid schemes. At high Reynolds numbers the accuracy of the spatial discretion of convective fluxes is a determining factor for both calculation accuracy and stability.

The continuity and momentum equations can be described in Cartesian tensor notation as follows:

- Equation of continuity

$$\frac{\partial}{\partial X_j}(\rho u_j) = 0 \tag{1}$$

- Equation of momentum

$$\frac{\partial}{\partial X_j}(\rho u_i u_j - \tau_{ij}) = \frac{\partial P}{\partial x_i} + S_i \tag{2}$$

- Equation of energy

$$\frac{\partial(\rho U_j T)}{\partial X_j} = \frac{\partial}{\partial X_j}\left[(\frac{\mu}{P_r} + \frac{\mu_t}{\sigma_r})\frac{\partial T}{\partial X_i}\right] \tag{3}$$

where ρ is the density of water and it is the velocity component. τij and Si denote the component of the stress tensor and momentum source respectively.

The particular high Reynolds number form the k-ε turbulence model used in the STAR-CD is 'appropriate', subject to the caveats given earlier, to fully turbulent, incompressible or compressible flows.

The governing equations for turbulent kinetic energy and dissipation in the Standard k-ε turbulence model are as follows :

- Equation of Turbulent kinetic energy

$$\frac{\partial}{\partial u_j}(\rho \bar{u}_j k - \frac{\mu_{eff}}{\sigma_k}\frac{\partial k}{\partial x_j}) =$$

$$\mu_t(P + P_B) - \rho\varepsilon - \frac{2}{3}(\mu_t \frac{\partial u_i}{\partial x_i} + \rho k)\frac{\partial u_i}{\partial x_i} + P_{NL} \tag{4}$$

where $P_{NL} = (-\overline{u_i u_j} - 2s_{ij})\frac{\partial u_i}{\partial x_j}$

- Equation of Turbulence dissipation rate

$$\frac{\partial}{\partial x_j}(\rho \bar{u}_j \varepsilon - \frac{\mu_{eff}}{\sigma_k}\frac{\partial \varepsilon}{\partial x_j}) =$$

$$C_{\varepsilon 1}\frac{\varepsilon}{k}\left[\mu_t(P + C_{\varepsilon 3}P_B) - \frac{2}{3}(\mu_t \frac{\partial u_i}{\partial x_i} + \rho k)\frac{\partial u_i}{\partial x_i}\right]$$

$$1 - C_{\varepsilon 2}\rho\frac{\varepsilon^2}{k} + C_{\varepsilon 4}\rho\varepsilon\frac{\partial u_i}{\partial x_i} + C_{\varepsilon 1}\frac{\varepsilon}{k}P_{NL} \tag{5}$$

where σε, Cε1, Cε2, Cε3 and Cε4 are empirical coefficients whose values, taken from references, are given in Table-3. The right-hand side terms represent similar effects to those described above for the k equation.

Table 3 Values assigned to standard k- ε turbulence model coefficients

| | | | |
|---|---|---|---|
| $C_\mu$ | 0.09 | $C_{\varepsilon 4}$ | -0.33 |
| $C_{\varepsilon 1}$ | 1.44 | $\sigma_k$ | 1.0 |
| $C_{\varepsilon 2}$ | 1.92 | $\sigma_\varepsilon$ | 1.22 |
| $C_{\varepsilon 3}$ | 0.0 or 1.0 | $\sigma_h$ | 0.9 |

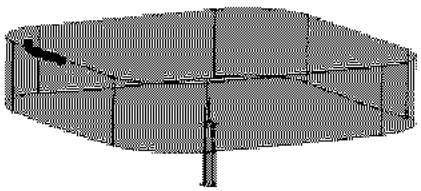

(a) Geometry of inland aquafarm

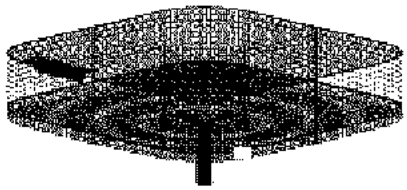

(b) Computational grid system of inland aquafarm

Fig. 3 Geometry and grid system for numerical analysis

The incoming Reynolds number is set to $2.12\times10^3$. The incoming temperature and atmosphere temperature are set to 293k and 283K, respectively. The vertical velocity was assumed to be 0, and turbulence intensity is set to 5% uniformly. The dynamic condition near the walls used wall function and adiabatic condition. The heat flux is

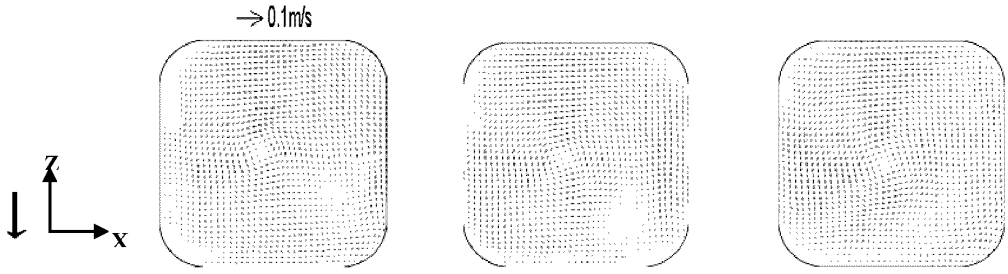


(a) Y=35mm (b) Y=25mm (c) Y=10mm

Fig. 4 Distributions of Velocity vectors for experimental results(X-Z plane, $Re=2.12\times10^3$)

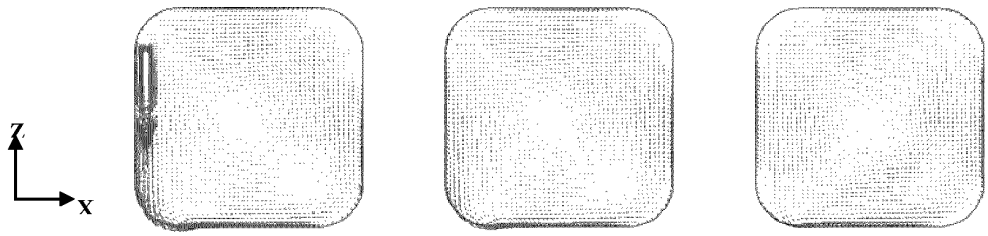


(a) Y=35mm (b) Y=25mm (c) Y=10mm

Fig. 5 Distributions of Velocity vectors for numerical analysis(X-Z plane, $Re=2.12\times10^3$)

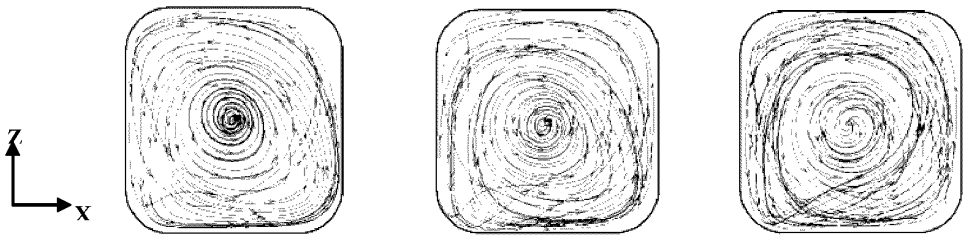


(a) Y=35mm (b) Y=25mm (c) Y=10mm

Fig. 6 Streamline for numerical analysis(X-Z plane, $Re=2.12\times10^3$)

set to $-20W/m^2$.

3D model calculation was performed using CATIA, and PRO-AM was used to create the lattice. The total number of lattices used for numerical modeling was 60,000. Actual calculation of the model used the common CFD code, STAR-CD ver-3.15A. Fig. 3(a) shows the measurement of inland aquafarm. The grid system of the numerical model is shown in Fig. 3(b). The calculation is repeated at steady state, and the iteration was assumed to be convergent when the residual value of the dependent variables was $10^{-3}$ or less.

## 3. Results & discussions

### 3.1 Comparisons of the experimental and numerical results

The general breeding fish inhabit near the bottom of a land aquaculture tank. The velocity distributions near bottom wall were found by selecting horizontal planes at different depths from top. Fig. 4 and 5 represent the velocity vectors of the experiment and numerical results respectively. The experimental and numerical results are compared for velocity difference, according to different X-Z planes at $Re=2.12\times10^3$.

Fig. 4 shows the time-averaged velocity vectors of the experimental results. Aquarium tank height from bottom are set to 10mm, 25mm and 35mm. The entire flow has a swirling flow pattern. The unique flow pattern appeared at near center. Velocity magnitude of this flow is decreased because the aquarium tank is shallow, and the velocity magnitude of walls are decreased by friction. Fig 4(b) shows the stagnation region at the corner of the right side. This is because of the

increased fluid velocity as the depth is decreased by X-Z plane at Re=2.12×10$^3$. The stagnation region is the smallest near the bottom which implies fluid flow is more stable at the bottom.

As the aquarium tank is shallow, the stagnation region is decreased to least area at the bottom of the aquarium tank.

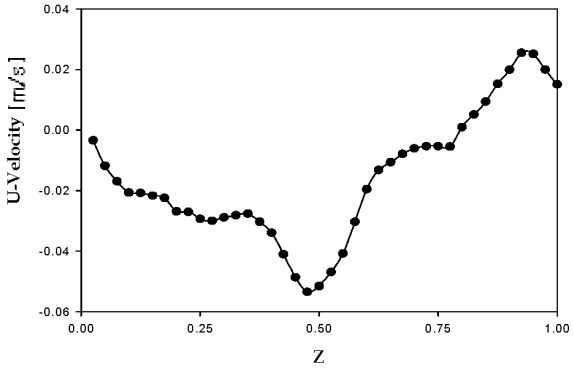


Fig. 7 Velocity distributions with Re=1.27×103 at X=100m and Y=10mm

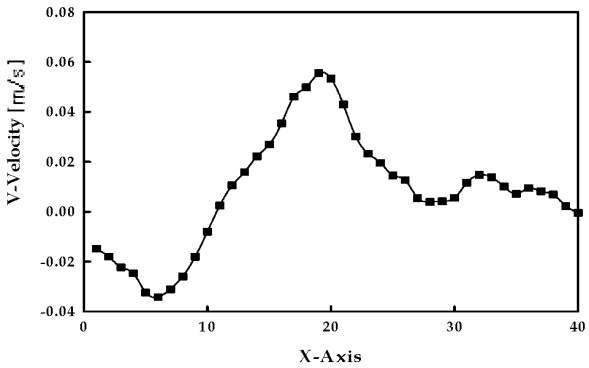


Fig. 8 Velocity distributions with Re=1.27×10$^3$ at Z=100mm and Y=25mm

Fig. 5 shows the time-averaged velocity vectors at the numerical analysis results. Fig. 5(a) shows that the velocity increases near the inlet as evident from the increased velocity vectors at Y=35mm near where the inlet is located. This is because the inlet velocity is streamed by a narrow pipe. In order to clarify the applicability of

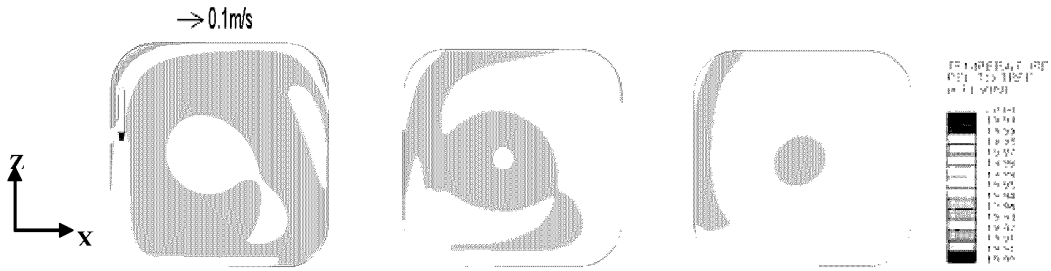


(a) Y=35mm (b) Y=25mm (c) Y=10mm

Fig. 9 Temperature contours for numerical results(X-Z plane, Re=4.23×102)

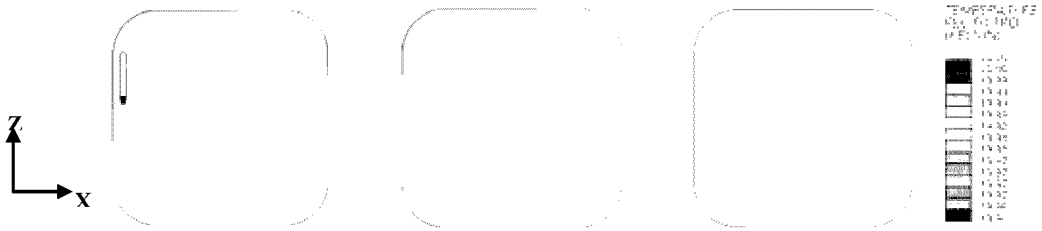


(a) Y=35mm (b) Y=25mm (c) Y=10mm

Fig. 10 Temperature contours for numerical analysis(X-Z plane, Re=1.27×103)

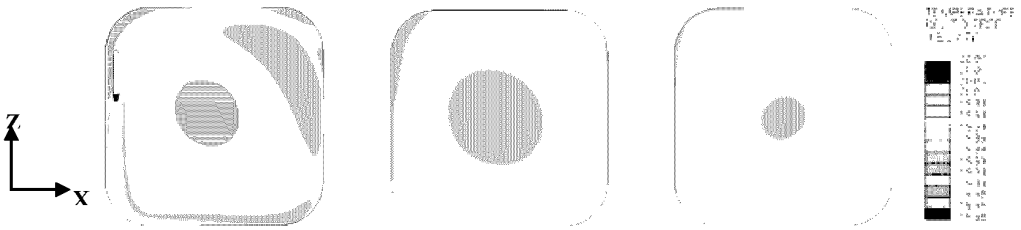


(a) Y=35mm (b) Y=25mm (c) Y=10mm

Fig. 11 Temperature contours for numerical analysis(X-Z plane, Re=2.12×103)

the foregoing numerical analysis, comparative studies with the experimental results have been carried out in an inland aquafarm model, and the calculated results had good agreements with the experiment. By comparing Fig. 4 and 5 the similarity of the experiment and numerical result can be observed.

Fig. 6 shows the streamline patterns at each section. The apparent swirl motion is observed in each section of the aquarium tank. As the depth is deeper, the swirl motion is advanced to right side the corner by outlet flow velocity. Consequently, at 10 millimeters depth the stagnation point at the near bottom right corner decrease. Therefore, this region can not cause the stagnation of pollutants and excrements, etc..

### 3.2 Temperature distributions of numerical analysis

As mentioned above, we analyzed and verified the flow field in an inland aquafarm model. One of the main purposes of this study is to obtain the flow and temperature profile in the actual aquaculture tank. In the aquaculture industry, the optimum temperature for breeding fish is about 2 0℃ in winter season. Thus, in this study, the size and temperature of the aquarium tank for calculation was set to the same conditions. In the case of an actual aquarium tank for breeding fish, the aquarium tank depth is not over 40mm. Therefore, the aquaculture tank depth selected was between 10 to 35mm. The costly breeding of fish in aquarium tanks is found to occur at near bottom of tank. Thus, the main flow characteristics were focused near the bottom in X-Z plane, Y=10mm.

Fig. 7 shows distributions of velocity with $Re=1.27\times10^3$. at X=100mm and Y=10mm. Fig. 8 shows distributions of velocity with $Re=1.27\times10^3$. at Z=100mm and Y=25mm. The surface of a wall at an inland Aquafarm approaches zero velocity by friction, the center appears maximum speed, meanwhile the bottom maintains stability flow.

## 4. CONCLUSION

In order to verify the calculation code, the numerical analysis and experimental PIV data were compared in the aquaculture tank model. Based on this calculation code, the flow field in the aquaculture tank was carried out for various tank geometry. Some important results can be summarized as follows.

1. The comparative studies with experimental results have been carried out, and the calculated results had good agreements with the experiment.
2. When the depth of the aquarium tank becomes deeper, the flow field near the bottom wall was advanced with stable flow and the stagnation region was least prominent. Therefore, this region can not cause the stagnation of pollutants and excrements which is good for fish breeding ,
3. As the depth of the aquarium tank is deeper, the high temperature appeared near the wall in the X-direction and Z-direction, and this high temperature is distributed widely due to large swirling flow.
4. The temperature in the aquarium tank is increased when the inlet velocity increases. This paper shows that the temperature of right down wall higher than inlet up side wall from $4.23\times10^2$ to $2,12\times10^3$.

## ACKNOWLEDGEMENT

This work was supported by the NURI Project and Korea Sea Grant Program by Ministry of Marine Affairs & Fisheries. The authors gratefully appreciate the supports.

## REFERENCES

[1] Kim, H. G. 1997, "Recent Harmful Algal Blooms and Mitgatio Stategies in Korea", Ocean Research, Vol.19, No.2, pp. 185-192.

[2] Partridge, B. L. 1989, "The Structure ad Function of Fish School, Sci. Am", Vol.246, pp. 90-99.

[3] Sannomiya, N. and Matuda, K, 1987, "Least

Squares Estmation in Fish Behavior Model", Bull. Japan. Soc. Sci. Fish. Vol. 53, pp. 1951-1957.

[4] Tsutomu Takagi, Kausuaki Nashimoto, Katsutaro Yamamoto and Tomonori Hiraishi, 1993, Kang, W. J., Cho, S. S., Huh, H. and Chung, D. T. 1998, "Identificatoin of Dynamic Behavior of Sheet Metals for an Auto-body with Tension Split Hopkinson Bar, SAE 981010", pp. 115-119.

[5] Jeong, H. M. and Chung, H. S, 1998, "Study on Fluid Flow Characteristics of Aquarium for Optimum Environment, Air-Conditioning and Refrigeration Engineering", Vol. 10, No. 1, pp. 108-117.

[6] Tomonori Hiraishi, Karsuaki Nashimoto, Thutomu Takagi, Kengo Suxuki and Keiichiro Moromatu, 1995, "Stationary Ability of Bastard Halibut Paralichthys olivaceus and Longsnout Flounder Limanda punctatissimato Water Current at the Bottom of a Net Cage, Bulletin of the Japanese Society of Scientific Fisheries", Vol. 61, No. 3, pp. 363-368.

[7] Lee, J. s, 1994, "Hydraulic Studies on Recirculating Aquaculture Basin, J. Korean Fish. Soc", Vol. 27, No. 2, pp. 173-182.

[8] Jones, W. P. and Launder, B. E, 1973, "The Calculation of Low-Reynolds-Number Phenomena with a Two-Equation Model of Turbulence, Int. J. Heat Mass Transfer", Vol. 16, pp. 1119-1130.

[9] Patel, V. C., Rodi, W. and Scheuerer, G,1985, "Turbulence Models for Near-Wall and Low Reynolds Number Flows, A Review, AIAA J ", Vol. 23, No. 9, pp. 1308-1319.

[10] Seo, H. T., Lee, D. S., Yoon, S. H. and Boo, J. S, 1998, "Numerical Analysis on Wall Attaching Offset Jet with Various Turbulent k-ε Models and Upwind Scheme, Trans", Of KSME, Part B, pp. 828-835.

[11] Patankar, S. V,1980, "Numerical Heat Transfer and Fluid Flow, Hemisphere Publishing corporation, McGraw-Hill, New-York".

[12] Daichin and Lee, S. J, 2003, "Evaluation of Recursive PIV Algorithm with Correlation Based Correction Method Using Various Flow Images, KSME International Journal", Vol. 17, No. 3, pp. 409-421.